Evolution Behavior of Hydrogen-Induced Nano Voids in AlZnMgCu Aluminum Alloys under Loading

Gao, Hongye
Department of Mechanical Engineering, Kyushu University

Su, Hang
Department of Mechanical Engineering, Kyushu University

Shimizu, Kazuyuki
Department of Mechanical Engineering, Kyushu University

Kadogawa, Chihiro
Department of Mechanical Engineering, Kyushu University

他

https://hdl.handle.net/2324/4485352

出版情報：MATERIALS TRANSACTIONS. 59 (9), pp.1532-1535, 2018-09-01. The Japan Institute of Metals and Materials
バージョン：

Materials Transactions, Vol. 59, No. 9 (2018) pp. 1532 to 1535

RAPID PUBLICATION

Evolution Behavior of Hydrogen-Induced Nano Voids in Al–Zn–Mg–Cu Aluminum Alloys under Loading

Hongye Gao[1], Hang Su[1,*], Kazuyuki Shimizu[1], Chihiro Kadokawa[1], Hiroyuki Toda[1],
Yasuko Terada[2], Kentaro Uesugi[2] and Akihisa Takeuchi[2]

[1]*Department of Mechanical Engineering, Kyushu University, Fukuoka 819-0395, Japan*
[2]*Japan Synchrotron Radiation Research Institute, Sayo-gun, Hyogo 679-5198, Japan*

Synchrotron X-ray nanotomography, which offers a state-of-the-art resolution, has been applied for the 3D observations of hydrogen induced nano voids under different strain levels in Al–Zn–Mg–Cu aluminum alloys. A great number of nano voids are initiated uniformly across the whole specimen during a loading process. The average diameter and number density of initiated nano voids is 300 nm and $5 \times 10^{15}\,\mathrm{m}^{-3}$, respectively. No evidence has been observed that the formation of nano voids results in the propagation of hydrogen induced quasi-cleavage cracks and premature fracture of Al–Zn–Mg–Cu aluminum alloys. Since nano void is one of the hydrogen trap sites in Al–Zn–Mg–Cu aluminum alloys, the majority of hydrogen can be repartitioned to nano voids during deformation due to their high density.
[doi:10.2320/matertrans.M2018156]

(Received May 8, 2018; Accepted June 8, 2018; Published August 25, 2018)

Keywords: *Al–Zn–Mg–Cu aluminum alloys, X-ray nanotomography, nanovoids, hydrogen trapping behavior*

1. Introduction

Al–Zn–Mg–Cu aluminum alloys have been drawn attention in the fields of structural materials due to its high specific strength and low cost compared to steels and titanium alloys.[1] Meanwhile, these alloys suffer from a limited ductility and unexpected premature fracture in aggressive environments such as moist air, sea water and hydrogen atmosphere due to their high hydrogen embrittlement susceptibility, which is treated as one of the key issues for the safe design and further improvement of Al–Zn–Mg–Cu aluminum alloys as an engineering material in the fields of aerospace, marine and nuclear industry.[2,3]

In recent years, a series of experiments and simulations have been applied to reveal the initiation and propagation of hydrogen-induced fracture and related hydrogen embrittlement behavior in metals.[4,5] Martin, *et al.* have revealed that nano voids initiated at the intersections of slip plane results in the propagation of hydrogen-induced quasi-cleavage cracks in pipeline steels in terms of hydrogen enhanced localized plasticity (HELP) model.[6] In contrast, Neeraj, *et al.* have revealed that the propagation of quasi-cleavage cracks is attributed to the coalescence of nano voids which is formed due to the stabilization and agglomeration of vacancies in the presence of hydrogen.[7,8] It can be inferred that nano voids play a significant role in the hydrogen embrittlement of metals, although there still exists a controversy on the formation and evaluation of nano voids in the presence of hydrogen. With the help of transmission electron microscopy (TEM), Su, *et al.* have observed the existence of hydrogen-induced nano voids in the strain localization region and proposed its influence on the repartitioning behavior of hydrogen among various trap sites during deformation in Al–Zn–Mg–Cu aluminum alloys.[9]

In the present research, the aim is to reveal the 3D evolution behavior of nano voids and related hydrogen repartitioning behavior within nano voids in Al–Zn–Mg–Cu aluminum alloys during deformation. Ultra-high-resolution X-ray nanotomography, which enables the visualization of the initiation, growth of each nano void, is applied to clarify the above issues.

2. Materials and Experimental Methods

In order to increase the strength of Al–Zn–Mg–Cu aluminum alloys, an aluminum alloy with chemical compositions of 10 mass% Zn, 2.4 mass% Mg, 1.5 mass% Cu, 0.05 mass% Fe and 0.05 mass% Si was applied for the present study. The heat treatment technology is T7651, specimens were homogenized at 743 K for 24 h and hot rolled at 473 K. Then, the rolled plates were solution treated at 748 K for 2 h, followed by water quenching and then artificially aged at 393 K for 6 h and then 423 K for 5 h.[10] *In-situ* tensile test specimens were sampled and hydrogen charged (Charged hydrogen content is 6.97 mass ppm) by an EDM (electro discharge machine) wire order. *In-situ* tensile tests via ultra-high-resolution X-ray nanotomography were performed with a photon energy of 20 keV at beamline BL37XU in SPring-8. The system was consisted of a beam diffuser, high precision stages, a center beam stop, a condenser zone plate (CZP), a Fresnel zone plate (FZP) and an X-ray image detector. The X-ray image detector is composed of a 2048 × 2048-element CMOS camera, a single-crystal scintillator (GdO_2S: Tb) and a lens. A series of radiographs were obtained every 0.1°, and the maximum rotation angle was 180°. Image slices were reconstructed by the conventional filtered back projection algorithm. The isotropic voxels in the reconstructed images were $(62\,\mathrm{nm})^3$ in size. The other details of the imaging procedure have been published elsewhere.[11]

3. Results and Discussion

3D observations of pre-existing hydrogen micro pores and nano voids under different strain levels are shown in Fig. 1. Both pre-existing hydrogen micro pores and nano voids are

---

[*] Corresponding author, E-mail: su.hang.844@m.kyushu-u.ac.jp

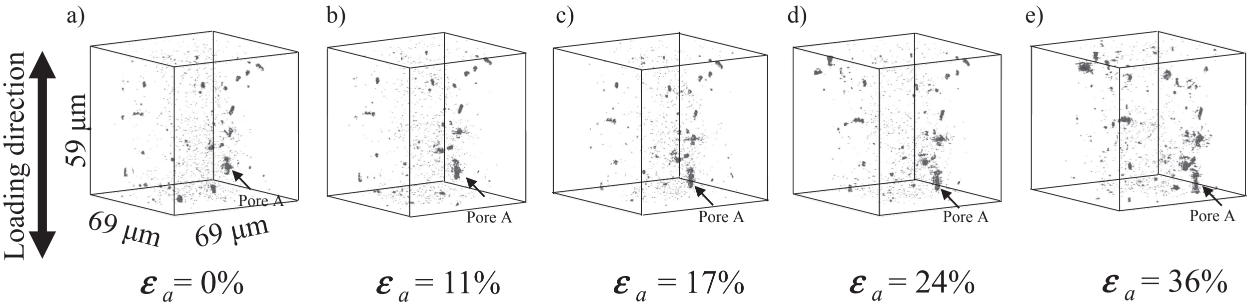

Fig. 1 3D reconstructed images of nano voids and pre-existing hydrogen micro pores in Al–Zn–Mg–Cu aluminum alloys under different applied strains: a) $\varepsilon_a = 0\%$, b) $\varepsilon_a = 11\%$, c) $\varepsilon_a = 17\%$, d) $\varepsilon_a = 24\%$ and e) $\varepsilon_a = 36\%$.

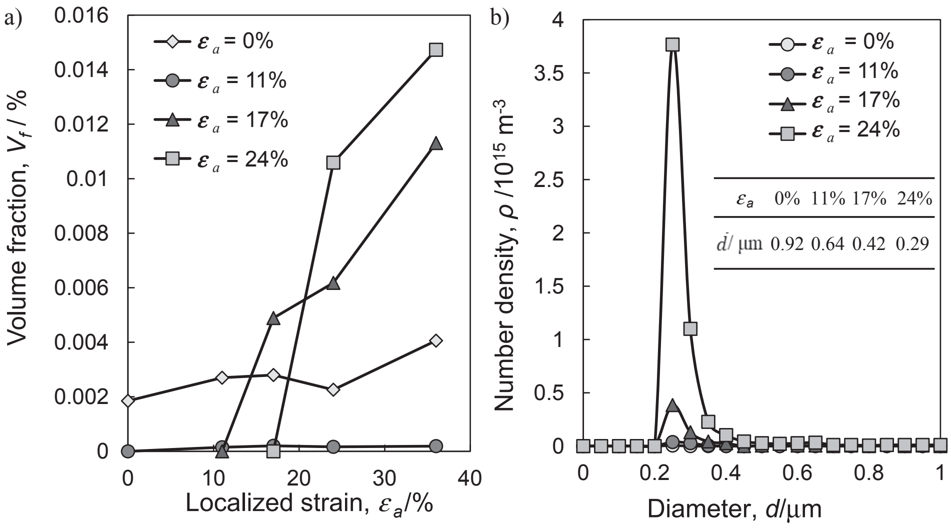

Fig. 2 a) Evolution of the volume fraction of newly initiated nano voids and b) the size distribution of nano voids under different strain steps ($\varepsilon_a = 0\%$, 11%, 17%, and 24%) in Al–Zn–Mg–Cu aluminum alloys.

observed at unloading state. Hydrogen micro pores are distributed heterogeneously in the matrix while nano voids are distributed uniformly across the whole specimen, as shown in Fig. 1(a). Turnbull, *et al.* have revealed that numerous hydrogen atoms are adsorbed into aluminum alloys and trapped at various trap sites such as dislocations, vacancies, particles and grain boundaries during the casting process due to the destruction of an oxide film.[12] Hydrogen micro pores are initiated heterogeneously on the intermetallic particles during the homogenization process.[9,13] In contrast, vacancies due to extensive plastic deformation are stabilized and agglomerated into nano voids in the presence of hydrogen during the rolling process.[14] During the *in-situ* tensile tests, it can be seen that nano voids are initiated uniformly across the whole specimen with an increase in applied strain levels, as shown in Fig. 1(b) to (e). In addition, hydrogen micro pores that heterogeneously initiated on particles induces strain concentration and high stress trixiality, which accelerates the growth of pre-existing hydrogen micro pores under loading, as shown as Pore A in Fig. 1. The growth of pre-existing hydrogen micro pore is consistent with the results that observed in both Al–Cu and Al–Mg aluminum alloys.[14,15)]

Microstructural tracking (MT) technique[16] has been applied for the analysis of the initiation and growth behavior of hydrogen-induced nano voids under different applied strain levels; the volume fraction and number density of nano voids during deformation is shown in Fig. 2. The volume fraction of pre-existing hydrogen micro pore and nano voids is approximately 0.002 at unloading state and remain stable during the applied strain ranges from 11% to 24%; the growth in volume fraction from 0.002 to 0.004 at an applied strain of 36% is mainly attributed to the coalescence of pre-existing hydrogen micro pores and voids at high strain levels, as shown in Fig. 1(e) and Fig. 2(a). In contrast, the volume fraction of hydrogen induced nano voids initiated at high applied strain levels ($\varepsilon_a = 17\%$ and 24%) is much higher compared to that of pre-existing hydrogen micro pores and nano voids and increases with an increase in applied strain levels, as shown in Fig. 2(a). The size distribution of the newly initiated nano voids is narrow, with a mean diameter of approximately 0.2 µm regardless of the applied strain levels, as shown in Fig. 2(b). Although the most frequency observed size range is not so different, numerous nano voids of approximately $3.7 \times 10^{15}\,\mathrm{m}^{-3}$ in number density are observed to be initiated at the strain of 24%. Due to the initiation of nano voids, the average diameter decreases with an increase in applied strain levels. No cluster or concentration of nano voids has been observed even in high strain levels, as shown in Fig. 1(e) and 2(b).

The 3D strain mapping observed along the *x*-*z* (RD-TD) virtual cross-section is shown in Fig. 3. The strain map reveals a highly heterogeneous strain in the strain

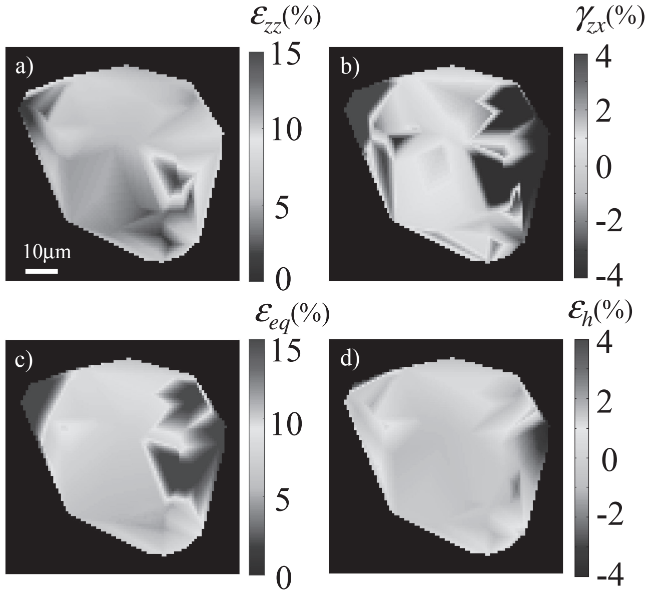

Fig. 3 3D strain maps of tensile tests between the 2nd ($\boldsymbol{\varepsilon}_a = 11\%$) and 3rd ($\boldsymbol{\varepsilon}_a = 17\%$) loading steps on an x-z virtual cross section: a) normal strain in the direction of loading, ε_{zz}, b) shear strain in the z-x direction, γ_{zx}, c) equivalent strain, ε_{eq} and d) hydrostatic strain, ε_h.

components of ε_{zz} and γ_{zx}, as shown in Fig. 3(a) and (b). Compared Fig. 3(c) with (d), it can be seen that regions of high hydrostatic strain appear to be located in the equivalent strain concentration region. Su, *et al.* have proposed that internal hydrogen tends to be accumulated in the equivalent strain concentration region during deformation.[13] Nagumo, *et al.* have revealed that vacancies are stabilized and agglomerated into nano voids in the presence of hydrogen.[17] Therefore, it can be inferred that the heterogeneous concentration of hydrostatic strain in the strain localization region might be attributed to the initiation of some invisible nano voids (<100 nm) due to localized vacancy concentration in the strain localization region. In addition, Su, *et al.* have revealed that the size of these nano voids in the hydrostatic strain concentration region is approximately 10 nm in size in Al–Zn–Mg–Cu aluminum alloys with the help of transmission electron microscopy (TEM).[9]

With the help of the X-ray nanotomography technique, it has been revealed that hydrogen-induced nano voids are initiated across the whole specimen during deformation in Al–Zn–Mg–Cu aluminum alloys. In steels, it has been reported that nano voids are initiated ahead of the crack tip and act as the propagation route of hydrogen induced quasi-cleavage cracks.[7,17] With the help of the transmission electron microscopy (TEM) and the first-principles simulation, Hachet, *et al.* have revealed that the formation of hydrogen-induced nano voids and hydrogen-vacancy culsters causes a degradation in mechanical properties of single crystal nickel alloys.[18] Unlike typical hydrogen-induced nano voids in steels and nickel alloys, numerous nano voids are formed uniformly during deformation in Al–Zn–Mg–Cu aluminum alloys. Neither the propagation of hydrogen-induced cracks nor the premature fracture that is attributed to the initiation and growth of nano voids has been observed in the present research.

On the other hand, nano void is one of the main hydrogen trap sites in aluminum alloys. Toda, *et al.* have reported that molecular hydrogen are trapped within nano voids;[19] Kirchheim, *et al.* have proposed that hydrogen atoms are adsorbed on the inner surfaces of nano voids.[20] Therefore, the total hydrogen content trapped within nano voids (C) is expressed as:

$$C = \theta_s N_s + 2n_g N_A \tag{1}$$

where θ_s is the trapped occupancy of adsorbed hydrogen, N_s is the number of hydrogen atoms adsorbed on the inner surface of nano voids per unit volume. N_A is the Avogadro's constant and n_g is the number of hydrogen molecules trapped within a hydrogen induced nanovoids, and is given by:

$$n_g = 4\gamma V/dRT \tag{2}$$

Where γ is the surface energy of aluminum, V is the volume of a nano void, d is the diameter of a nano void, R is the gas constant and T is the temperature. According to Kirchheim, *et al.*, the surface energy of aluminum is reduced due to the adsorption of hydrogen at the inner face of nano void:[20]

$$\gamma = \gamma_0 - (E_s + RTln\theta_L)N_s\frac{\theta_s}{N_A A} \tag{3}$$

where θ_L is the trapped occupancy of interstitial sites, θ_s is the trapped occupancy of nano voids and the binding energy of adsorbed hydrogen $E_s = 67.2\,\mathrm{kJ\,mol^{-1}}$ obtained through the first principles simulation[21] and A is the surface area of the inner surface of nano voids.

According to eq. (2) and (3), it can be inferred that the amount of adsorbed hydrogen atoms and molecule within nano void is influenced by the hydrogen trapped occupancy of interstitial lattice due to a thermal equilibrium among various trap sites,[22] as shown in Fig. 4. The content of adsorbed hydrogen atoms increases with an increase in trapped occupancy of interstitial lattice ranges from 1×10^{-16} to 1×10^{-11}; then remains at a value of approximately 5×10^{23} atomsH m^{-3}. In contrast, the content of molecular hydrogen decreases with an increase in trapped occupancy of interstitial lattice due to the decrease in the surface energy of nano voids, as shown in Fig. 3. Although the content of adsorbed hydrogen atoms decreases with a

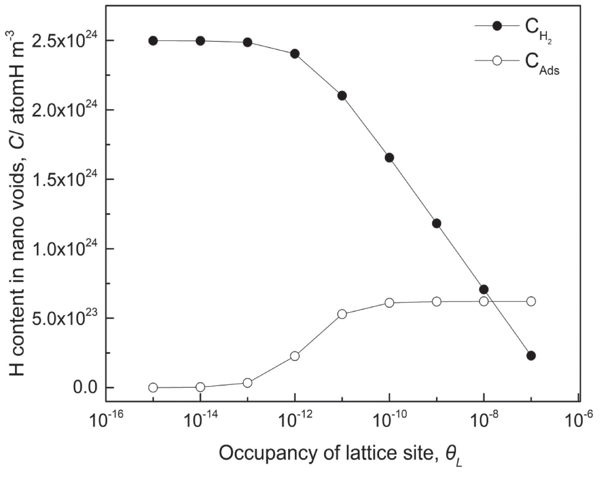

Fig. 4 Variations in hydrogen molecules and adsorbed hydrogen atoms trapped within nano voids corresponding to the occupancy of lattice sites.

decrease in trapped occupancy of interstitial lattice during the repartitioning process among various trap sites, it can still be obtained based on eq. (1) that the content of hydrogen trapped within nano voids increases from 0.02 mass ppm at unloading state to 0.44 mass ppm at an applied strain of 36% due to numerous formation of nano voids during deformation. In this approach, as a tensile strain is applied, numerous nano voids are homogeneously initiated in the matrix and both atomic and molecular hydrogen is trapped within nano voids, resulting in the repartitioning of hydrogen among various trap sites during deformation. In addition, it can be inferred that these newly nucleated nano voids directly affect the hydrogen repartitioning behavior in Al–Zn–Mg–Cu aluminum alloys, together with newly initiated dislocations and vacancies due to their high trap density during deformation.

4. Conclusion

In-situ tensile tests under the X-ray nanotomography show that nano voids nucleate dramatically during deformation in the presence of hydrogen. Since both hydrogen molecules and adsorbed hydrogen atoms are trapped within newly nucleated nano voids during loading, it can be inferred that repartitioning of hydrogen within nano voids during deformation is necessary to be considered for the occurrence of hydrogen induced premature fracture and related hydrogen embrittlement behavior.

Acknowledgments

The authors are grateful for the support of the Industry-Academia Collaborative R&D Program “Heterogeneous Structure Control” from the Japan Science and Technology Agency, JST. The synchrotron radiation experiments were performed at BL37XU of SPring-8 with the approval of the Japan Synchrotron Radiation Research Institute (JASRI) (Proposal Nos. 2016A1199 and 2016B1081).

REFERENCES

1) J.C. Williams and E.A. Starke, Jr.: Acta Mater. **51** (2003) 5775–5799.
2) R.G. Song, W. Dietzel, B.J. Zhang, W.J. Liu, M.K. Tseng and A. Atrens: Acta Mater. **52** (2004) 4727–4743.
3) I.W. Huang, B.L. Hurley, F. Yang and R.G. Buchheit: Electrochim. Acta **199** (2016) 242–253.
4) I.M. Robertson, P. Sofronis, A. Nagao, M.L. Martin, S. Wang, D.W. Gross and K.E. Nygren: Metall. Mater. Trans. A **46** (2015) 2323–2341.
5) H.K. Birnbaum and P. Sofronis: Mater. Sci. Eng. A **176** (1994) 191–202.
6) M.L. Martin, J.A. Fenske, G.S. Liu, P. Sofronis and I.M. Robertson: Acta Mater. **59** (2011) 1601–1606.
7) T. Neeraj, R. Srinivasan and J. Li: Acta Mater. **60** (2012) 5160–5171.
8) M. Nagumo, K. Ohta and K. Takai: Scr. Mater. **40** (1999) 313–319.
9) H. Su, H. Toda, R. Masunaga, K. Shimizu, H. Gao, K. Sasaki, M.S. Bhuiyan, K. Uesugi, A. Takeuchi and Y. Watanabe: Acta. Mater., Submitted.
10) H. Su, T. Yoshimura, H. Toda, S. Bhuiyan, K. Uesugi, A. Takeuchi, N. Sakaguchi and Y. Watanabe: Metall. Mater. Trans. A **47** (2016) 6077–6089.
11) H. Toda, K. Uesugi, A. Takeuchi, K. Minami, M. Kobayashi and T. Kobayashi: Appl. Phys. Lett. **89** (2006) 143112.
12) A. Turnbull: Int. J. Hydrogen Energy **40** (2015) 16961–16970.
13) H. Su, S. Bhuiyan, H. Toda, K. Uesugi, A. Takeuchi and Y. Watanabe: Scr. Mater. **135** (2017) 19–23.
14) H. Toda, H. Oogo, K. Horikawa, K. Uesugi, A. Takeuchi, Y. Suzuki, M. Nakazawa, Y. Aoki and M. Kobayashi: Metall. Mater. Trans. A **45** (2014) 765–776.
15) H. Toda, H. Oogo, K. Uesugi and M. Kobayashi: Mater. Trans. **50** (2009) 2285–2290.
16) M. Kobayashi, H. Toda, Y. Kawai, T. Ohgaki, K. Uesugi, D.S. Wilkinson, T. Kobayashi, Y. Aoki and M. Nakazawa: Acta Mater. **56** (2008) 2167–2181.
17) M. Nagumo: Mater. Sci. Technol. **20** (2004) 940–950.
18) G. Hachet, A. Metsue, A. Oudriss and X. Feaugas: Acta Mater. **148** (2018) 280–288.
19) H. Toda, T. Hidaka, M. Kobayashi, K. Uesugi, A. Takeuchi and K. Horikawa: Acta Mater. **57** (2009) 2277–2290.
20) R. Kirchheim, B. Somerday and P. Sofronis: Acta Mater. **99** (2015) 87–98.
21) M. Yamaguchi, K. Ebihara, M. Itakura, T. Tsuru, Y. Shiihara, K. Matsuda and H. Toda: Comput. Mater. Sci., Submitted.
22) R.A. Oriani: Acta Mater. **18** (1970) 147–157.